New Journal of Chemistry

Electronic Supplementary Information

An anthracene-quinoline based dual-mode colorimetric/fluorometric sensor for detection of Fe^{3+} and its application in live cell imaging

Tahereh Tehrani [a], Soraia Meghdadi [a□], Zohreh Salarvand [b], Behnam Tavakoli [a], Kiamars Eskandari[a] and Mehdi Amirnasr [a□]

[a] *Department of Chemistry, Isfahan University of Technology, Isfahan 8415683111, Iran*

[b] *Department of Chemistry, Chemistry and Petrochemistry Research Center, Institute of Standard and Industrial Research of Iran (ISIRI), Karaj 3174734563, Iran*

Corresponding authors: M. Amirnasr, S. Meghdadi

**E-mail addresses*: amirnasr@cc.iut.ac.ir

smeghdad@cc.iut.ac.ir

Amirnasr ORCID: 0000-0002-4232-2097

Meghdadi ORCID: 0000-0002-2597-9521

Table of Contents **Page**

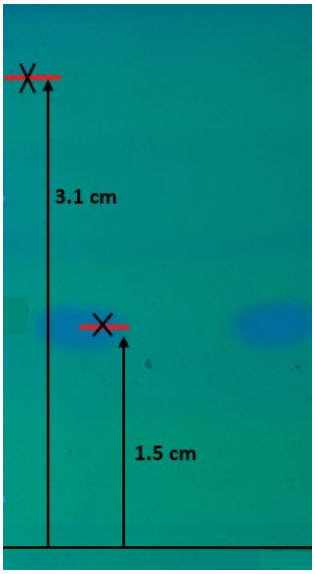

$$R_f = \frac{1.5}{3.1} = 0.48$$

Fig. S1. The retardation factor (R_f) of **HAQ** in EtOAc/Hexan, 30/70.

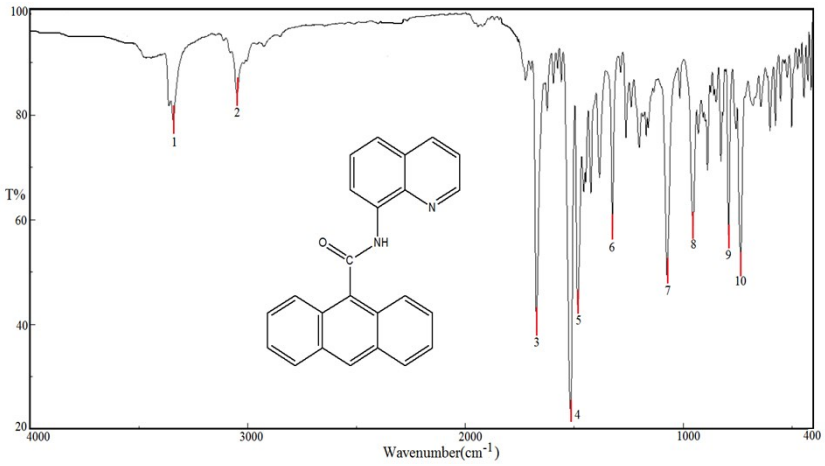

Result of peak picking

No.	cm-1	%T	No.	cm-1	%T	No.	cm-1	%T
1	3343	43.1602	2	3052.76	48.2893	3	1672.95	28.2712
4	1516.74	16.8293	5	1483.96	31.4983	6	1324.86	42.7445
7	1074.16	37.7972	8	953.627	45.7512	9	790.671	45.3878
10	734.746	41.3309						

Fig. S2. FT-IR spectrum of the chemosensor **HAQ** (KBr pellet).

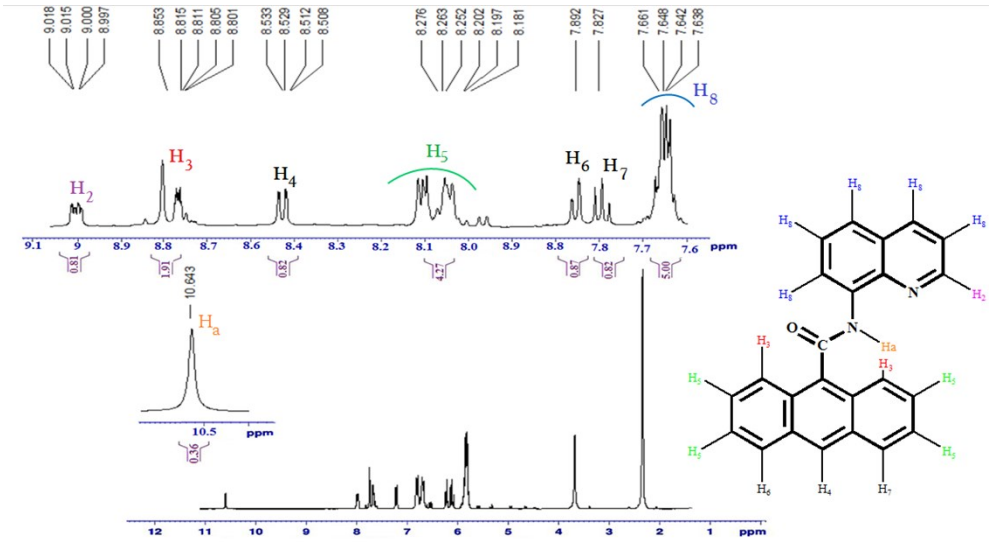

Fig. S3. ^{1}H NMR spectrum of the chemosensor **HAQ** in DMSO-d_6 at room temperature.

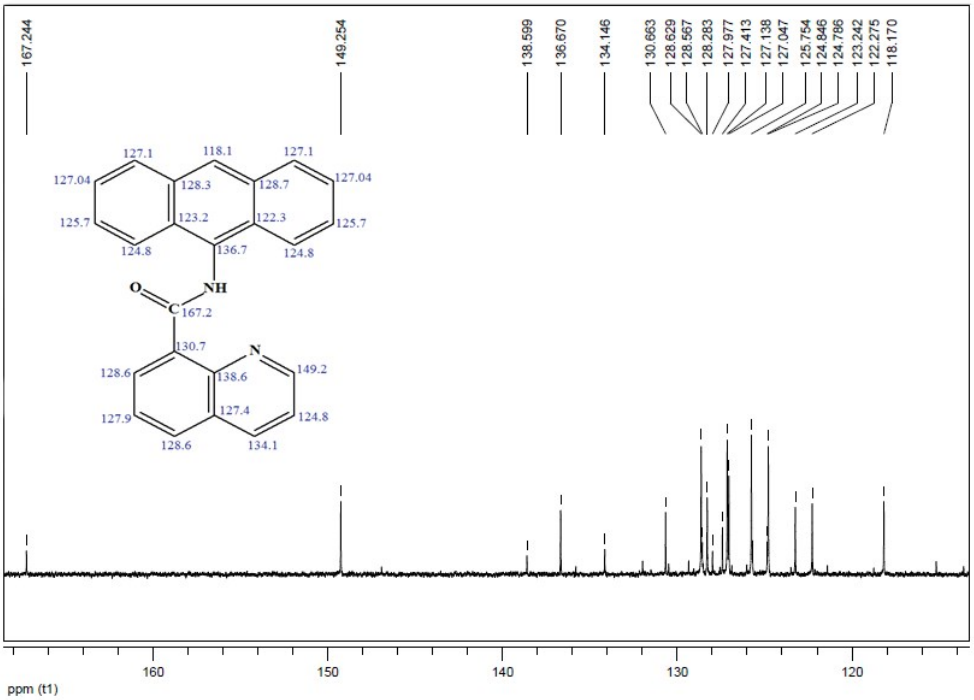

Fig. S4. ^{13}C NMR spectrum of the chemosensor **HAQ** in DMSO-d_6 at 293.5 K.

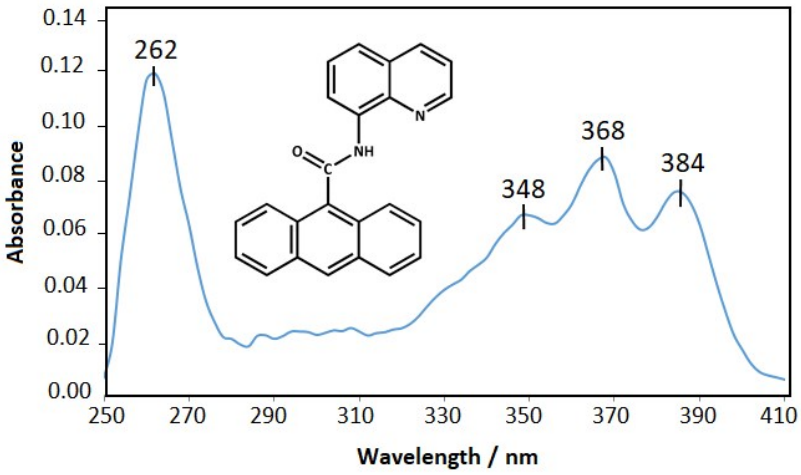

Fig. S5. Absorption spectra of HAQ in DMSO (1.0×10^{-5} M) at room temperature.

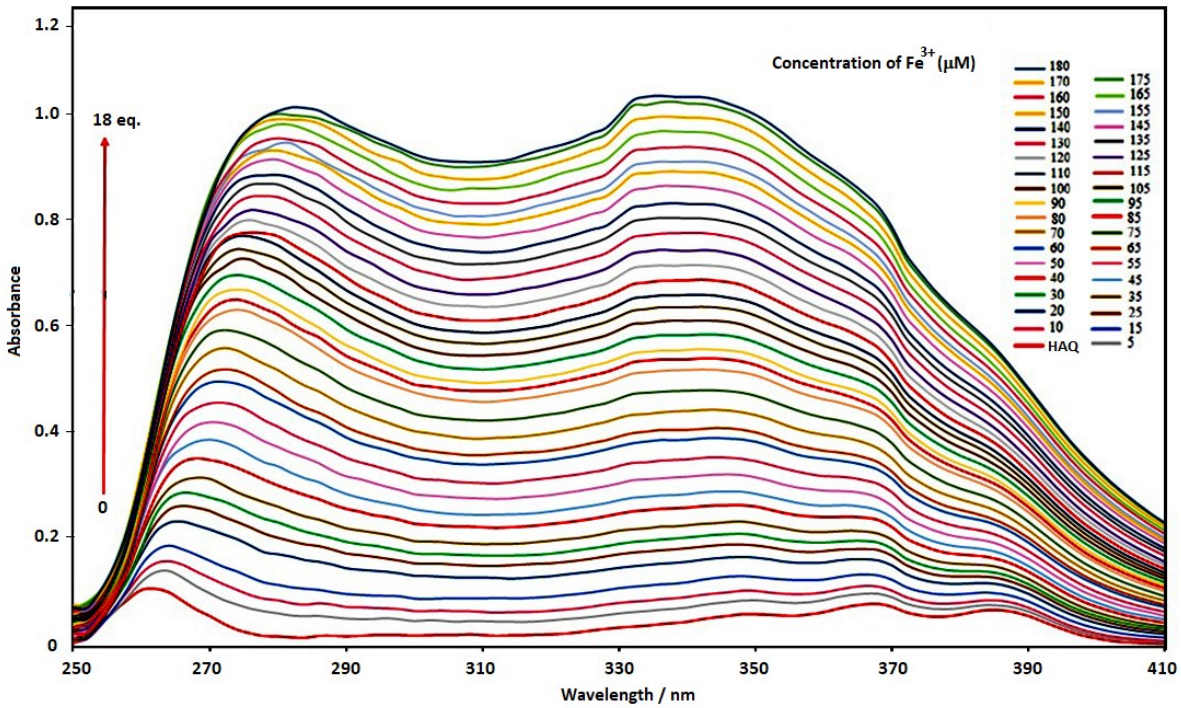

Fig. S6. Changes in the absorption spectrum of **HAQ** (1.0×10^{-5} M) in the presence of increasing concentration (0−180 μM) of Fe^{3+} ion in a DMSO solution.

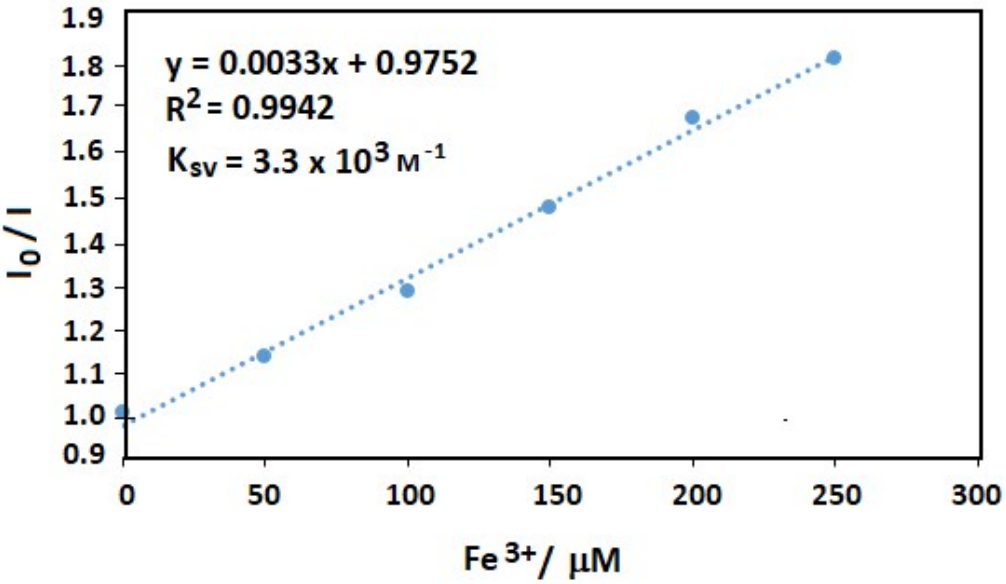

Fig. S7. Stern-Volmer plot obtained from **HAQ** titration with Fe^{3+}. Ksv = 3.3×10^3 M^{-1}.

Determination of LOD for HAQ as Fe^{3+} chemosensor.

$[Fe^{3+}]$/μM	Average Fl.	STDEV
0	970.88	0.87899
50	941.342	0.87379
100	837.879	0.87364
150	727.642	0.86638
200	618.634	0.86265
250	490.741	0.85867
300	395.634	0.82821
350	327.64	0.80976
400	254.562	0.80375

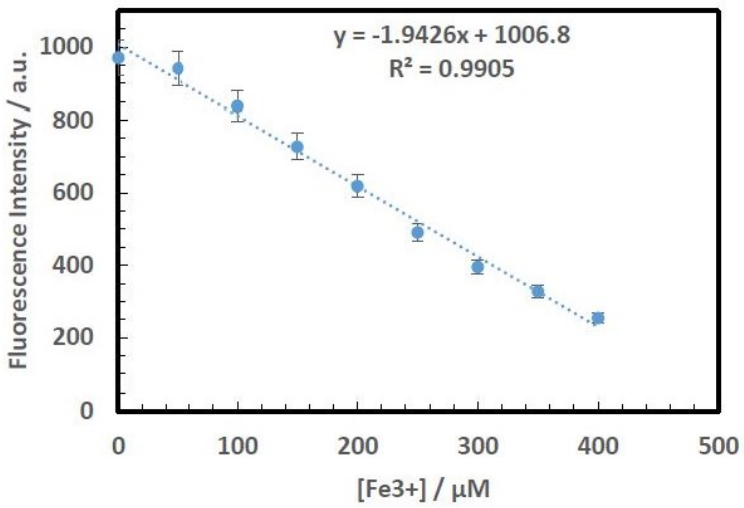

$[Fe^{3+}]$/μM	Fl. Intensity at λ_{ex}
0	964.071
0	965.526
0	966.031
0	964.608
0	964.271
0	965.954
0	966.536
0	964.284
0	964.9
0	965.541
Average	965.172
STDEV	0.86132

S = -Slope=1.9426 μM^{-1}

STDEV=σ = $\sqrt{\frac{\Sigma(F-\bar{F})^2}{(N-1)}}$ =0.86132 (N = 10)

LOD = 3*σ/S = 1.33 μM =1.3 * 10^{-6} M

Fig. S8. The fluorescence spectrum linear range of **HAQ** (50 μM) at 386 nm upon addition of Fe^{3+}.

Determination of binding constant for Fe^{3+} complex using Benesi–Hildebrand equation.

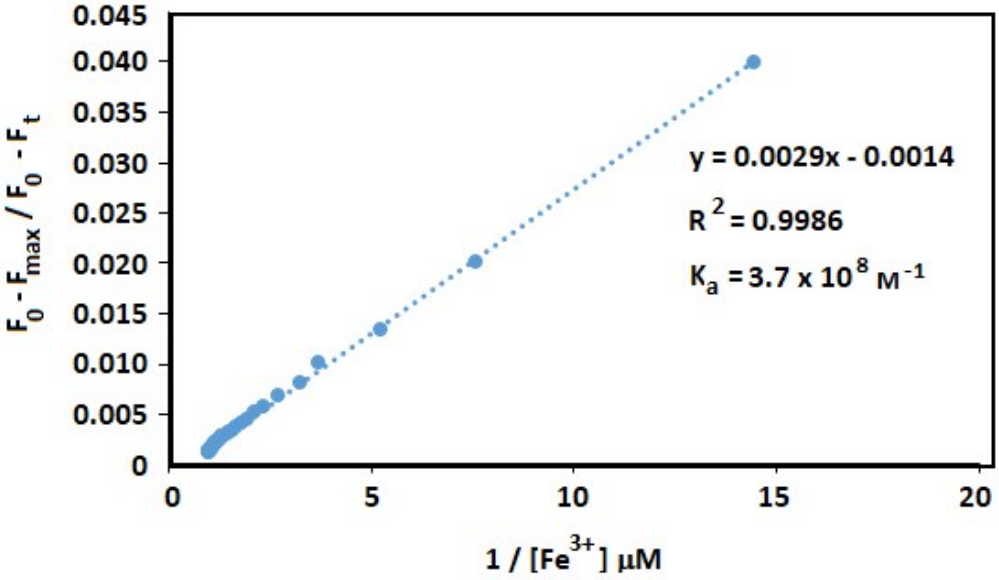

Fig. S9. The Association constant (K_a) of **AQ**-Fe^{3+} complex.

$1/(F_0 - F_t) = 1/(K_a \times (F_0 - F_{max}) \times [Fe^{3+}]) + 1/(F_0 - F_{max})$

$K_a = 3.7 \times 10^8\ M^{-1}$

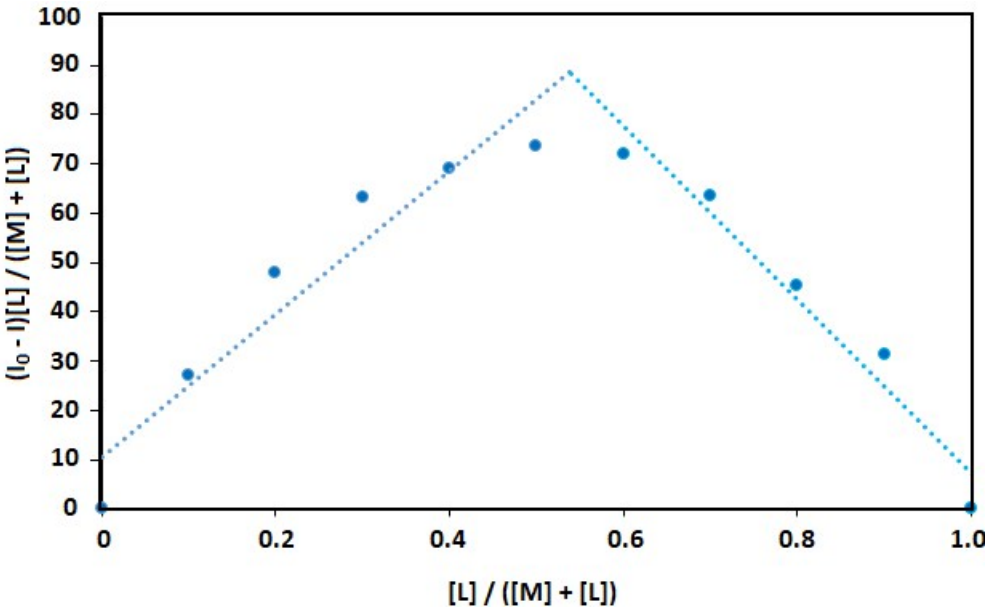

Fig. S10. Job's plot of the **AQ**-Fe^{3+} complex in DMSO, with the monitoring wavelength set at 486 nm.

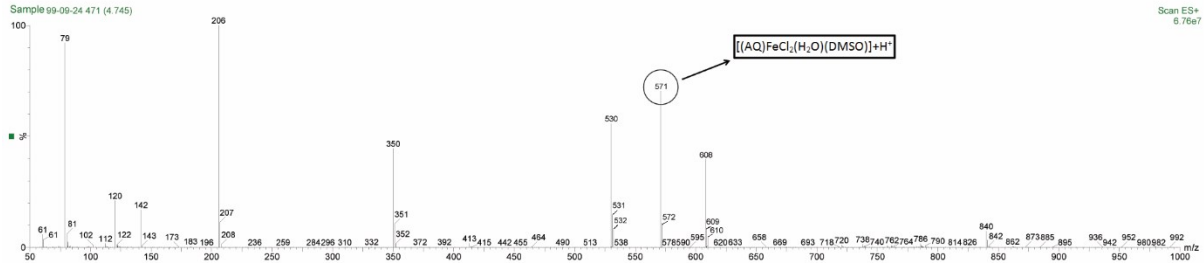

Fig. S11. ESI-MS spectrum for **AQ**-Fe^{3+} in DMSO with the peak at m/z = 571.00 corresponding to {[(**AQ**)$FeCl_2(H_2O)$(DMSO)] + H^+} (calculated m/z = 571.30).

X-ray crystallography of HAQ

Colorless crystals of **HAQ** suitable for X-ray crystallography were obtained by slow evaporation of solution of the ligand in CH_2Cl_2-CH_3OH (4:3 v/v) at room temperature. X-ray data of the **HAQ** were collected on a Stoe IPDS-2T diffractometer with graphite monochromated Mo Kα (λ = 0.71073 Å) radiation. Data were collected at 296(2) K in a series of ω scans in 1° oscillations and integrated using the Stöe X-AREA 1.43 software package.[1] The structure was solved by direct methods using SHELXTL-2008.[2] The non-hydrogen atoms were refined anisotropically by the full-matrix least-squares method on F^2 using the SHELXTL program.[2] The hydrogen atoms were treated by a mixture of independent and constrained refinements. Details of crystallographic data and refinements of the HAQ chemosensor are summarized in Table S1. CCDC 2003356 contains the supplementary crystallographic data for this paper. These data can be obtained free of charge from The Cambridge Crystallographic Data Centre via www.ccdc.cam.ac.uk/data_request/cif.

1 X-AREA, version 1.30, program for the acquisition and analysis of data, Stoe & Cie GmbH, Darmstadt, Germany, 2005.
2 G.M. Sheldrick, Acta Crystallogr. Sect. A 64 (2008) 112-122. DOI: 10.1107/S0108767307043930.

Table S1. Crystal data and structure refinement for chemosensor **HAQ**.

Chemical formula	$C_{24}H_{16}N_2O$
M_r	347.62
T (K)	296(2)
λ (Å)	0.71073
Crystal system, space group	Triclinic, $P\bar{1}$
a (Å)	8.8312(18)
b (Å)	16.467(3)
c (Å)	24.385(5)
α (°)	89.63(3)
β (°)	87.94(3)
γ (°)	89.72(3)
V(Å^3)	3543.8(12)
Z, D_{calc} (Mg/m^3)	2, 1.303
Crystal size (mm)	0.21 × 0.11 × 0.07
μ (mm^{-1})	0.081
F(000)	1450
Θ ranges (°)	2.61-29.64
Absorption correction	Multi-scan
Reflections collected/unique/R_{int}	15362/ 11915/ 0.095
Data/restrains/parameters	11915/0/877
Refinement method	Full-matrix least-squares on F^2
$R[F^2 > 2\sigma(F^2)]$, $wR(F^2)$, S	0.057, 0.109, 0.50
Goodness-of-fit on F^2	0.504
Final R indices [I>2σ(I)]	$R1$ = 0.4154, $wR2$ = 0.1089
R indices (all data)	$R1$ = 0.0565, $wR2$ = 0.0691
H-atom treatment	H-atoms treated by a mixture of independent and constrained
$\Delta\rho_{max}$, $\Delta\rho_{min}$ (e Å^{-3})	0.136, -0.125

Table S2. Selected bond lengths (Å) and angles (°) for chemosensor **HAQ.**

Bond lengths		*Bond angles*	
C(11)-O(1)	1.207(14)	O(1)-C(11)-N(1)	126.5(9)
N(1)-C911)	1.426(16)	O(1)-C(11)-C(12)	128.0(13)
N(1)-C(1)	1.382(9)	N(1)-C(11)-C(12)	105.5(10)
C(11)-C(12)	1.578(10)		

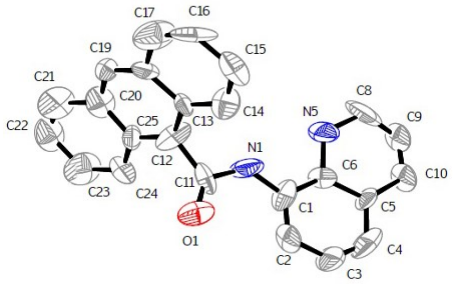

HAQ

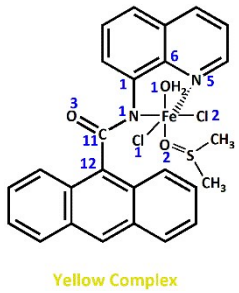

[(**AQ**)$FeCl_2(H_2O)$(DMSO)]

Table S3. Bond lengths (Å) and bond angles (°) of HAQ and [(**AQ**)$FeCl_2(H_2O)$(DMSO)] complex.

Compund	*Bond lengths*		*Bond angles*	
	Experimental	Theoretical	Experimental	Theoretical
HAQ	C(11)-O(1) 1.207(14)	1.228	O(1)-C(11)-N(1) 126.5(9)	124.3
	C(11)-N(1) 1.426(16)	1.364	O(1)-C(11)-C(12) 128.0(13)	121.7
	C(1)-N(1) 1.382(9)	1.402	N(1)-C(11)-C(12) 105.5(10)	114.1
	C(6)-N(5) 1.488(11)	1.361	C(6)-C(1)-N(1) 116.2(11)	115.0
			C(1)-C(6)-N(5) 121.4(9)	118.0
	Bond lengths	Theoretical	*Bond angles*	Theoretical
AQ-Fe Complex	N(1)-Fe	2.101	N(1)-C(1)-C(6)	117.2
	N(5)-Fe	2.206	N(5)-C(6)-C(1)	117.4
	H_2O(1)-Fe	2.230	C(1)-N(1)-C(11)	116.9
	Cl(1)-Fe	2.331	N(1)-C(11)-C(12)	118.7
	Cl(2)-Fe	2.455	N(1)-Fe-O(1)	86.0
	O(2)-Fe	2.022	N(1)-Fe-O(2)	95.9
	N(1)-C(1)	1.405	N(5)-Fe-O(1)	86.5
	N(1)-C(11)	1.388	N(5)-Fe-O(2)	88.0
	C(11)-O(3)	1.232	Cl(1)-Fe-O(1)	90.6
	C(11)-C(12)	1.508	Cl(1)-Fe-O(2)	94.6
			Cl(2)-Fe-O(1)	82.5
			Cl(2)-Fe-O(2)	94.1
			N(5)-Fe-Cl(1)	175.9
			N(5)-Fe-Cl(2)	87.0
			N(1)-Fe-Cl(1)	105.2
			N(1)-Fe-Cl(2)	161.2
			Cl(1)-Fe-Cl(2)	89.7
			O(1)-Fe-O(2)	173.7
			N(1)-Fe-N(5)	77.5
			C(6)-N(5)-Fe	112.6
			C(1)-N(1)-Fe	114.6

MO	Complex	E (eV)	SPIN
	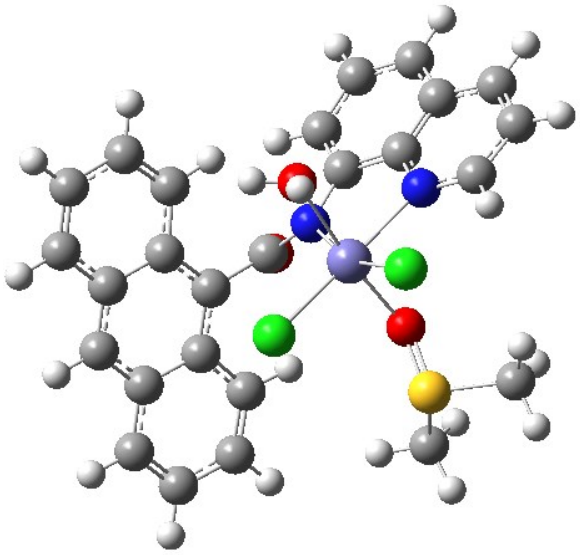	--	--
LUMO+7	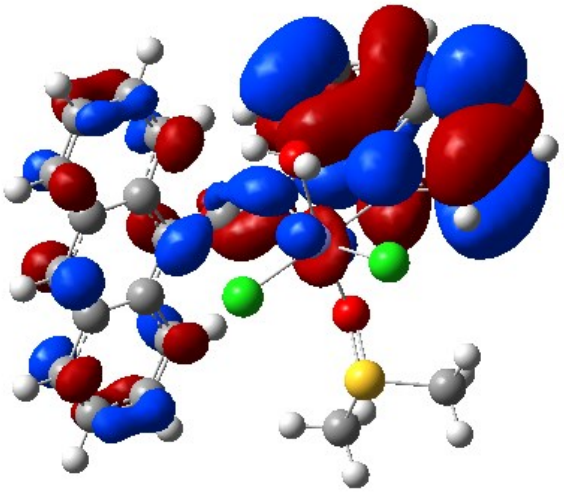	-2.12	--

LUMO+6	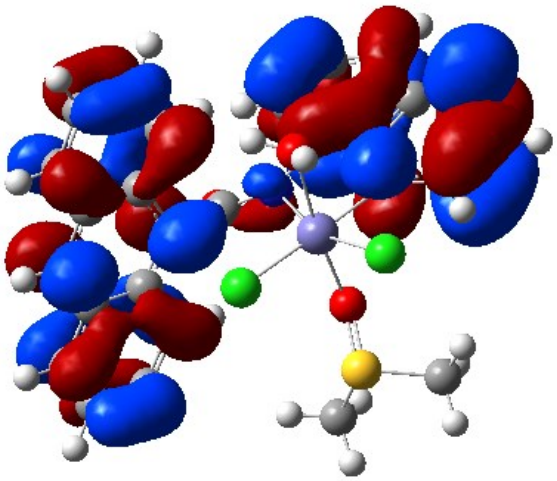	**-2.21**	**--**
LUMO+5	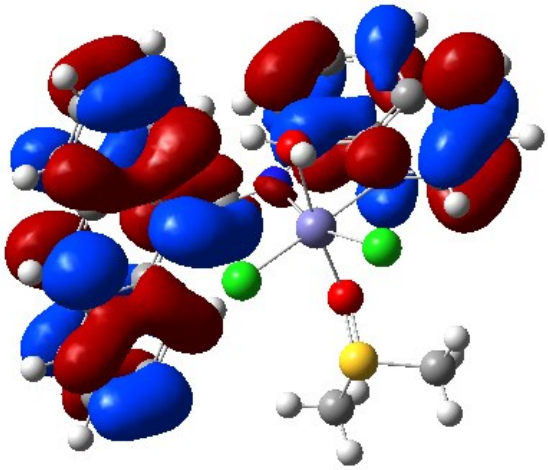	**-2.33**	**--**
LUMO+4	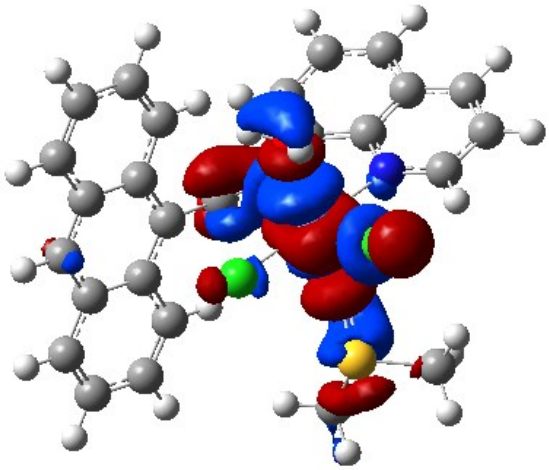	**-2.61**	**--**

LUMO+3	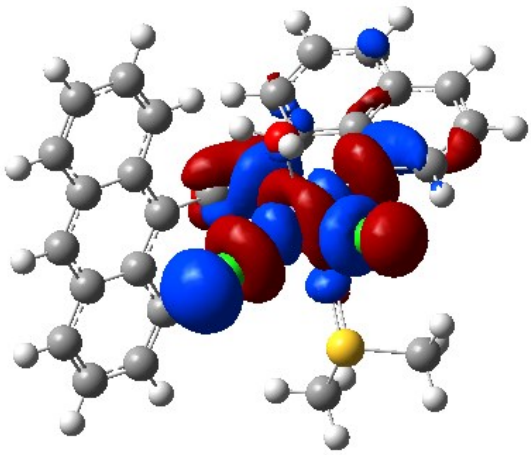	**-2.67**	**--**
LUMO+2	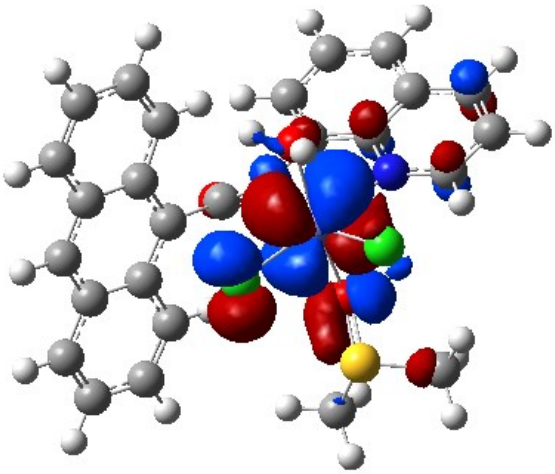	**-3.60**	**--**
LUMO+1	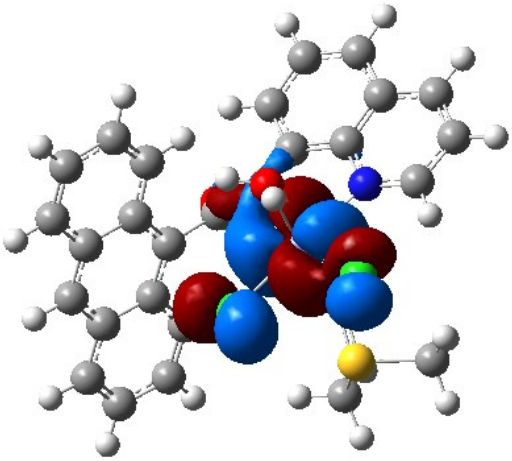	**-3.65**	**--**

LUMO	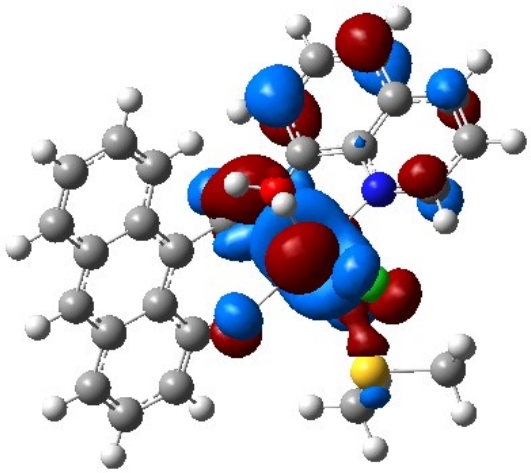	**-3.93**	**--**
HOMO	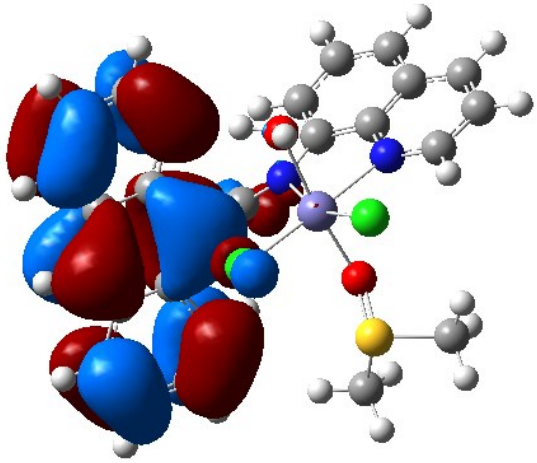	**-5.71**	**β**
HOMO-1	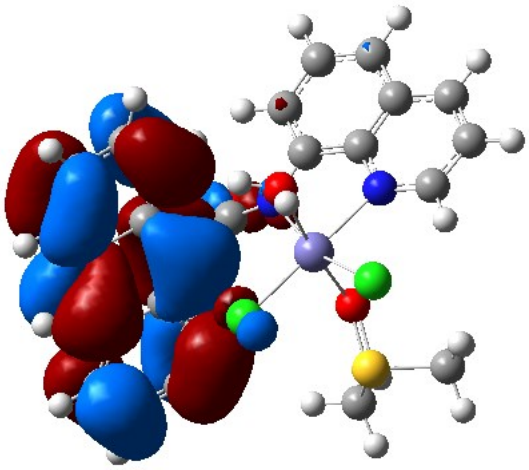	**-5.72**	**α**

HOMO-2	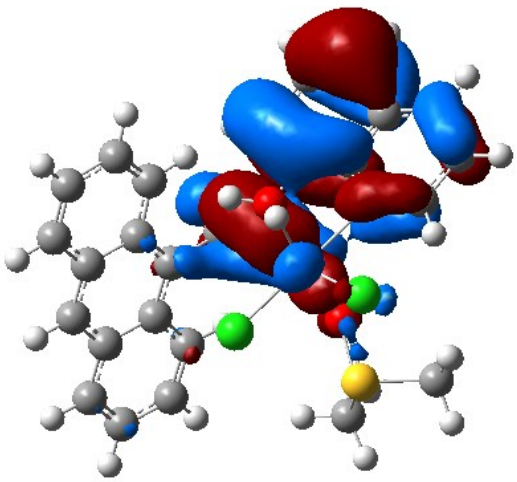	**-6.03**	**β**
HOMO-3	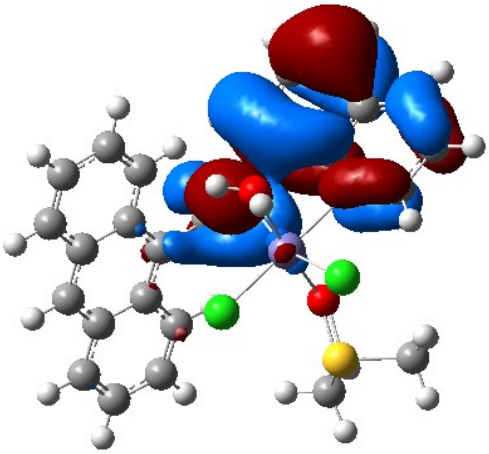	**-6.07**	**α**
HOMO-4	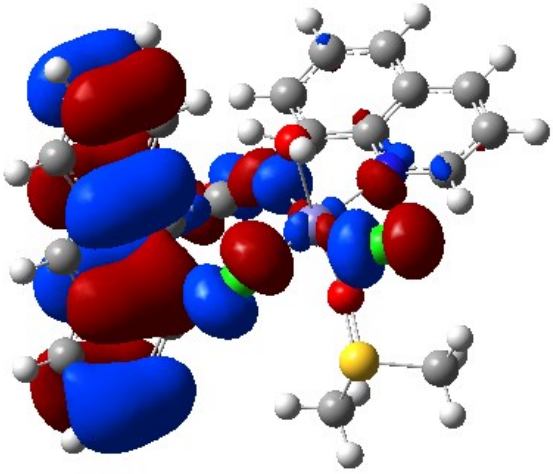	**-6.93**	**α**

HOMO-5	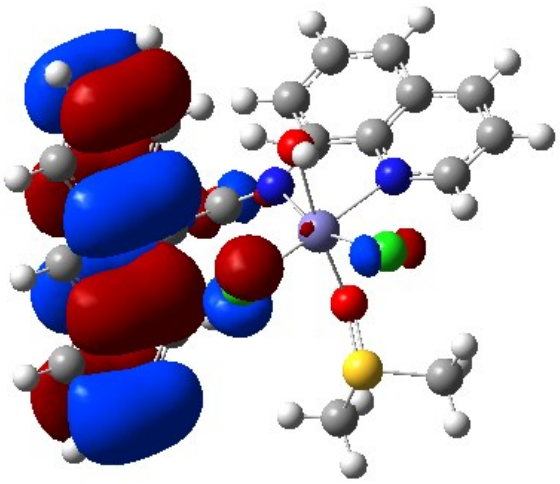	**-6.95**	**β**
HOMO-6	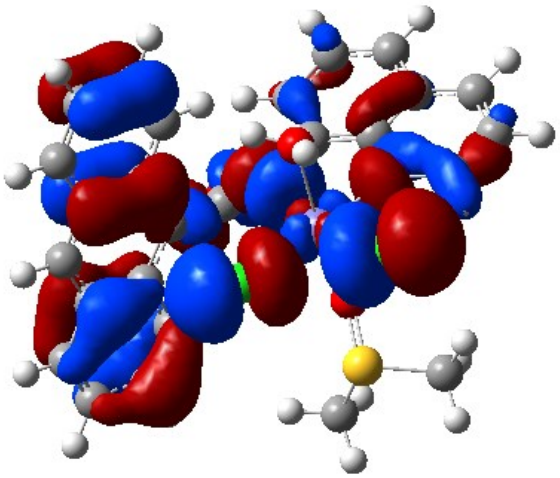	**-7.05**	**α**
HOMO-7	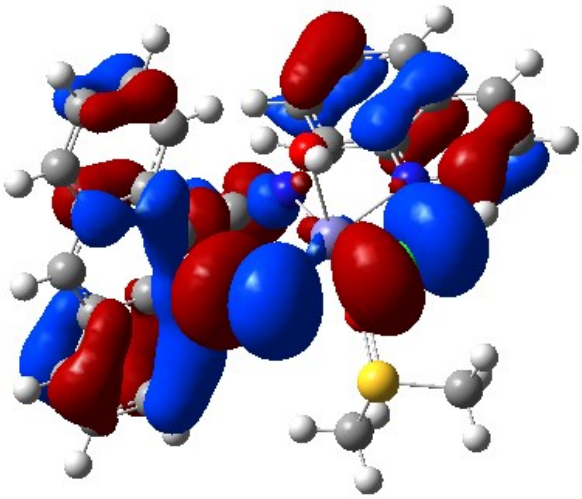	**-7.17**	**β**

HOMO-8	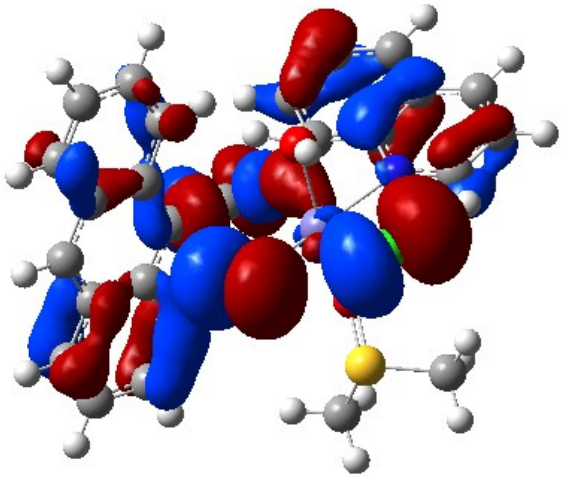	**-7.25**	**β**
HOMO-9	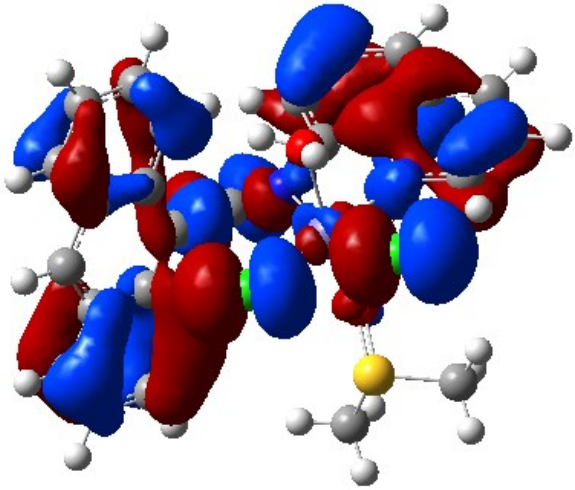	**-7.30**	**α**
HOMO-10	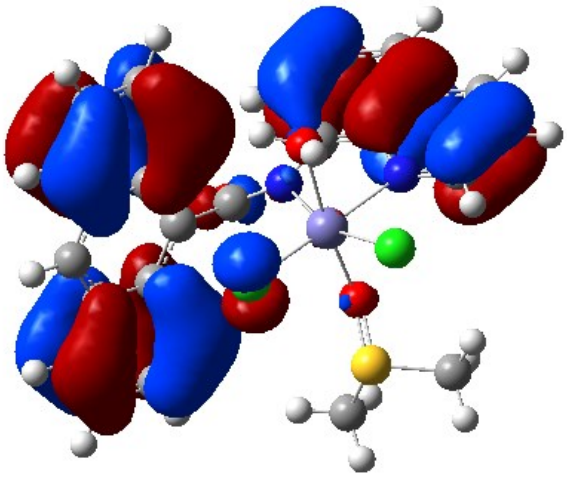	**-7.41**	**β**

HOMO-11	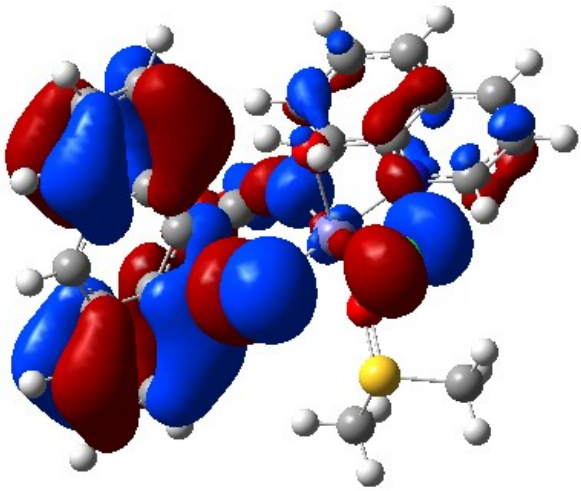	**-7.41**	**α**
HOMO-12	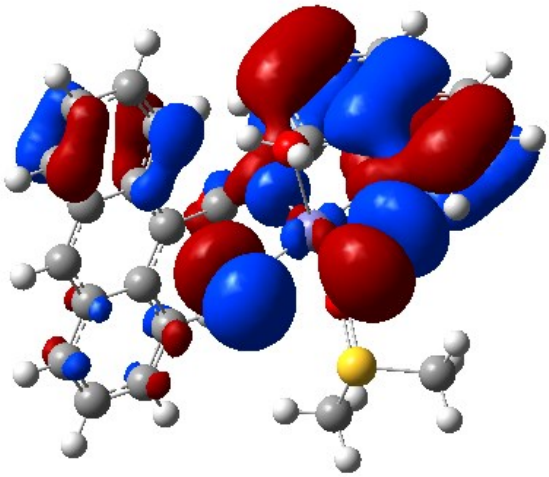	**-7.43**	**α**
HOMO-13	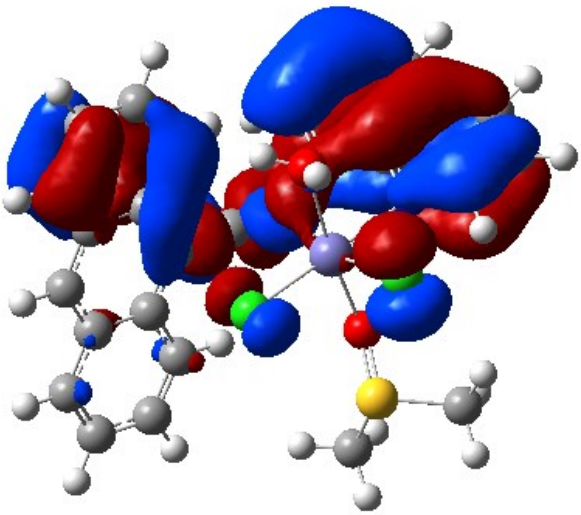	**-7.51**	**β**

HOMO-14	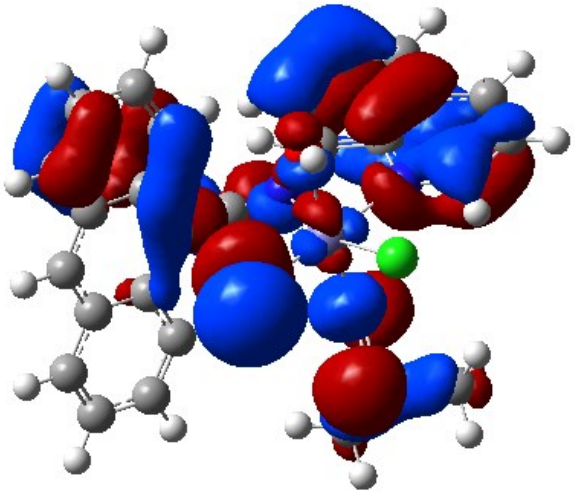	**-7.57**	**α**
HOMO-15	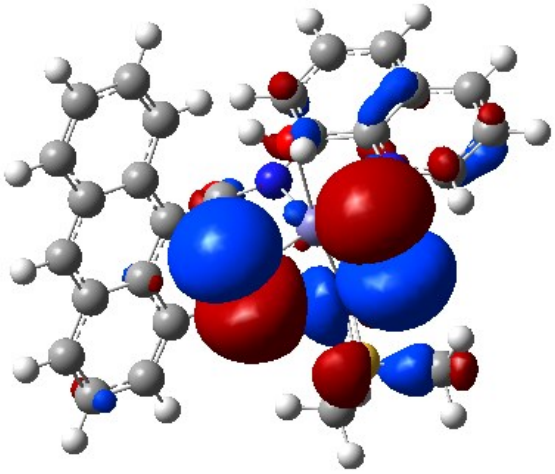	**-7.66**	**β**
HOMO-16	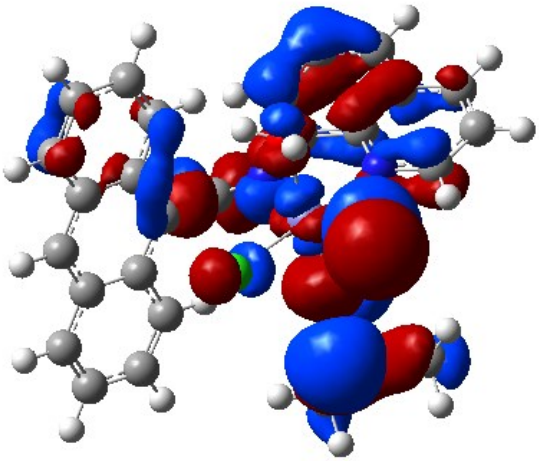	**-7.66**	**α**

HOMO-17	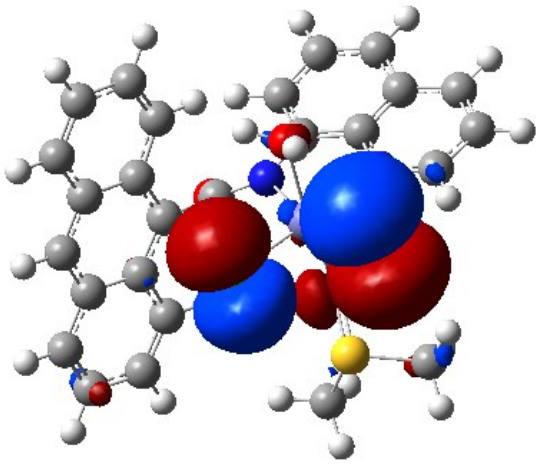	**-7.78**	**α**
HOMO-18	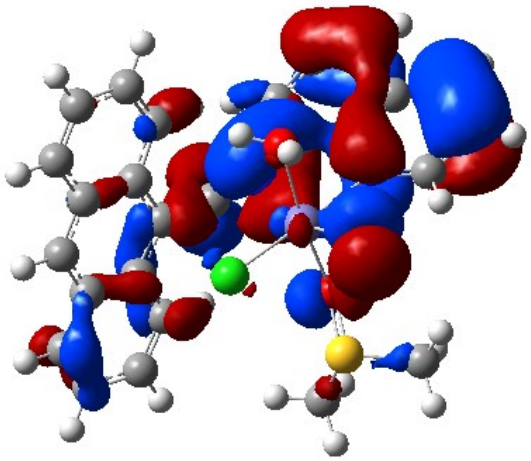	**-7.84**	**β**
HOMO-19	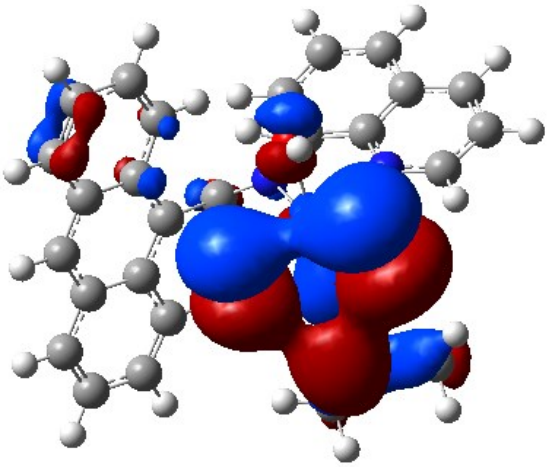	**-7.86**	**β**

HOMO-20	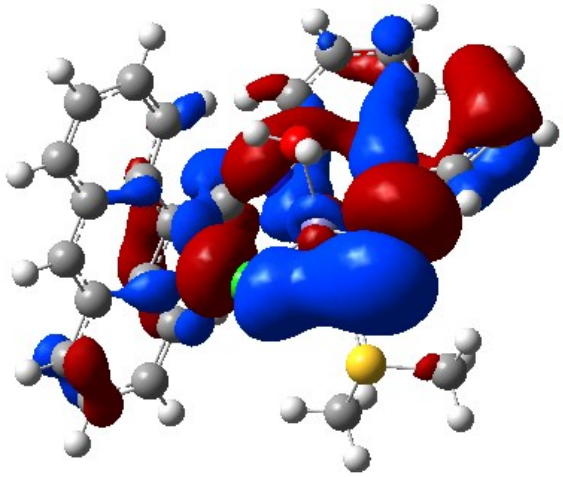	**-7.89**	**α**

MO	**HAQ**	**E (eV)**
	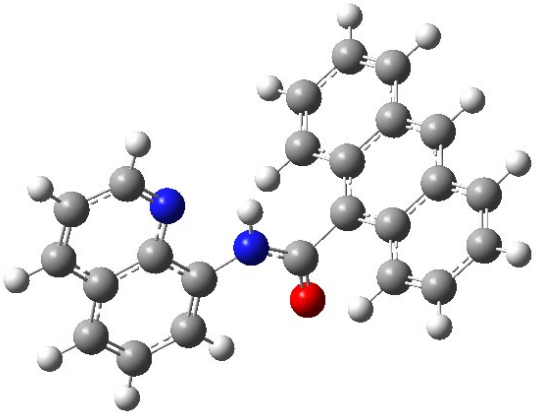	

LUMO+1	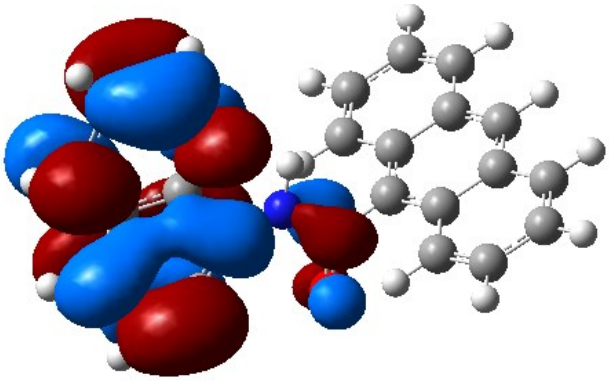	**-2.04**
LUMO	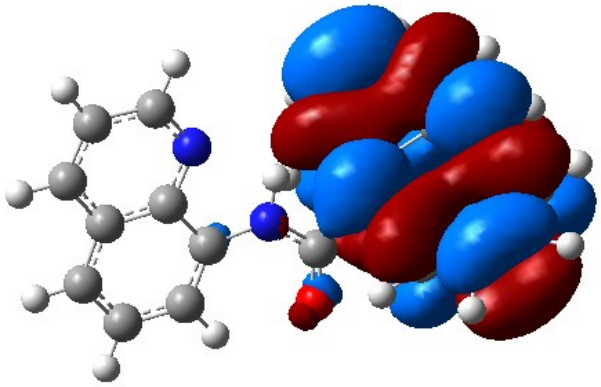	**-2.30**
HOMO	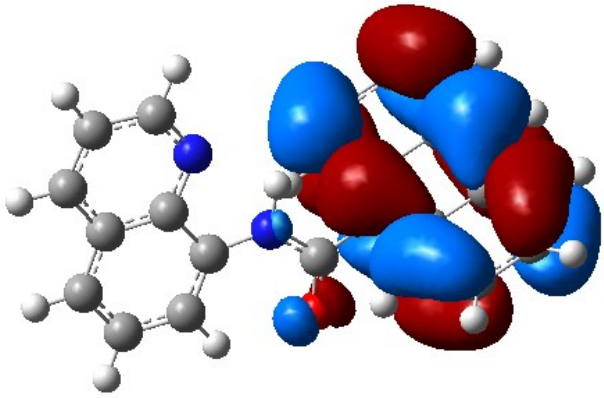	**-5.81**

HOMO-1	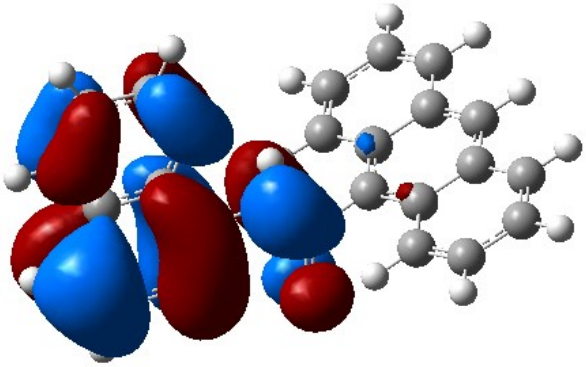	**-6.32**

Fig. S12 Structures and Profiles of frontier molecular orbitals of the **HAQ** and [(**AQ**)$FeCl_2(H_2O)$(DMSO)].